韓國鑛物學會誌 第 10 卷 第 2 號 (1997)
J. Miner. Soc. Korea, 10, 126-138 (1997)

Serpentinization of the Ultramafic Rock in the Yesan-Gongju-Cheongyang Area, Korea

충남 예산-공주-청양지역의 초염기성암의 사문암화 작용

Geon-Young Kim (김건영) · Soo Jin Kim (김수진)

Department of Geological Sciences, Seoul National University, 151-742, Seoul, Korea
(서울대학교 지질과학과)

ABSTRACT : Serpentinite of the Yesan-Gongju-Cheongyang area has been formed by serpentinization of ultramafic rocks. The ultramafic rock might be composed mainly of olivine with minor pyroxene and amphibole. Olivine has a considerably restricted chemical compositional ranging from Fo_{90} to Fo_{93}. Fresh serpentinite containing large amount of olivine is usually massive in occurrence and dark green to black in color. Serpentine minerals occur not only as major mineral of serpentinite, but also as remnants in the talc ore which was formed from serpentinite. XRD study indicates that antigorite is the most abundant serpentine mineral of the serpentinite. Serpentinite consisting of antigorite usually shows non-pseudomorphic texture, whereas that consisting of lizardite shows pseudomorphic texture. Antigorite is found along the margins or fractures of olivine grains resulting in the formation of network of magnetite which was formed at the time of serpentinization. Lizardite, subordinate constituent mineral of serpentinite, frequently shows pseudomorphic mesh-texture after olivine. The chemical differences between antigorite and lizardite/chrysotile are small, so both minerals are not easily discernible with the electron microprobe. Antigorite occurs as elongate blades, flakes, or plates forming interpenetrating texture to obliterate previous textures. SEM study also shows that most serpentine minerals occur in platy or tabular form rather than in asbestiform. Fractures formed after main serpentinization are observed within the pseudomorphic central olivine grain. Careful observation of the serpentine pseudomorphs gives a great deal of data on the pre-serpentinization nature of the ultramafic rocks. It is inferred that the serpentinization took place after the emplacement of ultramafic body into the relatively wet environment ceased and the cooling intrusive body crossed into the stability field of serpentine. It is inferred that the final pervasive serpentinization took place over a long time, by hydrothermal water supplied through the fracture system produced during emplacement of ultramafic rock.

요약 : 예산-공주-청양지역의 활석광상에서 산출되는 사문암은 이 지역 초염기성암이 사문암화작용을 받아서 생성되었다. 초염기성암은 주로 감람석과 소량의 휘석류 및 각섬석류로 구성되었을 것이다. 감람석은 사문석의 모광물로서 Fo_{90}-Fo_{93}에 해당하는 화학조성을 보인다. 주로 감람석으로 구성된 신선한 사문암은 보통 어두운 녹색이나 검은색의 괴상으로 산출된다.
사문석은 사문암의 주구성광물로 뿐만 아니라 활석광석내에 잔존물로 산출되기도 한다. X-선 회절분석결과 연구지역에서 양적으로 가장 우세하게 산출되는 사문석 광물은 앤티고라이트 이며 이들은 주로 감람석입자 주변 및 내부균열을 따라 생성되었고, 감람석의 원래 입자형태를 따라 자철석이 망상으로 산출되기도 한다. 리자다이트는 그물구조를 이루며 주로 감람석의 가상으로 산출된다. 앤티고라이트와 리자다이트/크리소타일 간의 화학분석치에서의 차이는 거의 없어서 이에 의한 구분은 매우 어렵다. 주로 앤티고라이트로 구성된 사문석은 가상조직을 보이

지 않으나 리자다이트로 구성된 사문암은 가상조직을 보여준다. 앤티고라이트는 길게 신장된 엽상이나 판상으로 산출되며 서로 침투된 밀집구조를 보이기 때문에 모광물의 가상구조가 보이지 않는다. 주사전자현미경 관찰결과 대부분의 사문석광물은 침상보다는 판상으로 산출된다. 사문암화작용시기 이후에 생성된 것으로 보이는 균열들이 가상내에 잔류하는 감람석 입자에서 관찰된다. 가상을 이루고 있는 사문석의 조직연구는 사문암화작용 이전의 초염기성암에 관한 많은 정보를 주고 있다. 일단 초염기성암이 상대적으로 수분을 많이 함유하고 있는 주변암에 관입한 후 냉각되기 시작하여 사문석광물의 안정영역에 도달하게 되었을 때 초염기성암을 구성하고 있는 감람석과 휘석류의 사문암화작용이 진행되었다. 초염기성암 전체에 대한 광역적인 사문암화작용은 초염기성암이 관입하면서 생성시킨 균열대를 따라 열수가 지속적으로 공급되면서 가속되었을 것으로 추정된다.

INTRODUCTION

Serpentine minerals are predominent constituents of many ultramafic rocks, but little is known about details of their formation. In general, serpentines are known to be formed by pseudomorphic replacement of olivine and phlogopite (Mitchell, 1986; Sharp et at., 1990), late-stage crystallization from the melt, or alteration of primary minerals (Mitchell and Putnis, 1988; Jago and Mitchell, 1985). Most talc deposits in the Yesan-Gongju-Cheongyang area were originated from ultramafic rocks.

Obviously, ultramafic rocks that have been highly serpentinized are not suitable for the detailed study of their original textures prior to serpentinization. However, Boyd and Nixon (1979) shows that even in highly serpentinized olivine the outlines of the primary grain-boundaries are preserved, and Laurent and Hebert (1979) have observed the pseudomorphic replacement of olivine and enstatite by lizardite in harzburgite tectonites.

Even though no relict of original ultramafic rocks of pre-serpentinization is found and most serpentinites are altered to talc-chlorite rock by steatitization in the study area, the least altered serpentinites contain some original texture of parent minerals. In addition, although fresh serpentinites are not abundantly found, some of them often show pseudomorphic texture of parent silicates, in which the parent grain boundaries are preserved. The pseudomorphic process not only preserves the outline of the original grains and the original textures, but also it preserves the fracture patterns and cleavages of the parent minerals (Wicks, 1984). Considerable amounts of information on the pre-serpentinization history can be found despite complete serpentinization. Therefore, this paper is focussed on the characterization of serpentine minerals of the study area and their mineralogical and textural relation to the serpentinization of the ultramafic rocks.

GEOLOGICAL SETTING

The Yesan-Gongju-Cheongyang talc mining area consists nearly entirely of Precambrian granitic gneiss with minor hornblende gneiss, tremolite schist, serpentinite, and dike rocks in the restricted mining area. The granitic rocks were formed by regional metamorphism of both epidote-amphibolite and later greenschist facies and granitization (Lee and Choi, 1994). Talc mineralized zones are generally developed as elongate or lens-shaped bodies in the Precambrian granitic gneiss (Fig. 1). The Daeheung, Pyeongan, and Shinyang talc mines are three representative mines in the northeast trending mineralized zone developed over the area of about 6 to 7km in length and 10 to 100m in width. There are little differences in mineralogy and occur-

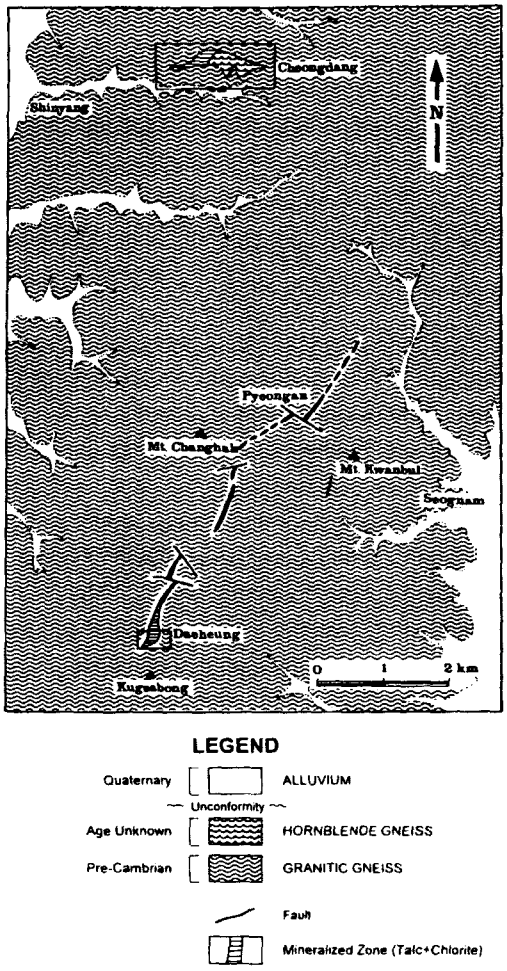

Fig. 1. Geologic map of the Yesan-Gongju-Cheongyang area.

rence of the talc ores among three talc mines. The major constituent minerals of the talc ores are talc, chlorite, phlogopite, amphibole, serpentine minerals such as antigorite and lizardite, and carbonates and the minor minerals are olivine, pyroxene, chromite, smectite, and some other expandable clay minerals such as regularly interstratified smectite/chlorite (corrensite).

Detailed geologic map of the Daeheung mine was prepared from the open pits over a wide area (Fig. 2). Many acidic or basic dikes are found in the area. Tremolite schist

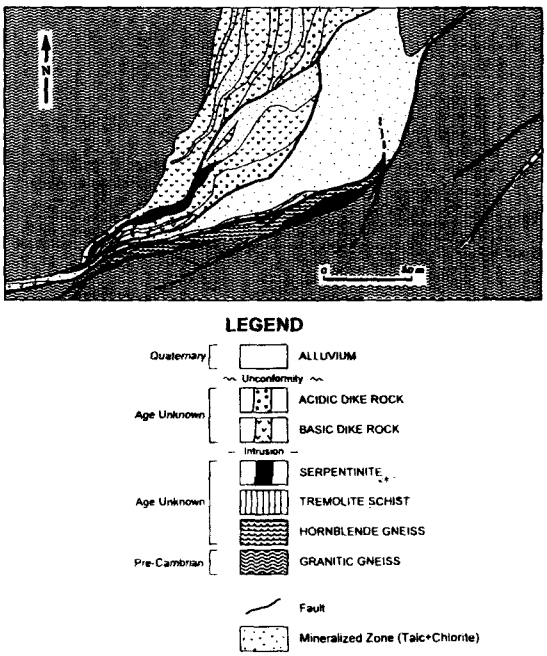

Fig. 2. Detailed geologic map of the open pit of the Deaheung Mine.

and hornblende gneiss are also found along the margin of the talc ore bodies. Unaltered serpentinite relicts are present within talc ore bodies. Serpentinite which has partly altered to talc is also often observed. The occurrence of fresh serpentinite in the talc ore body is a good evidence for the ultramafic origin of the talc deposits. Under the microscope, olivine is also found as relicts in serpentinite.

EXPERIMENTAL METHODS

Preliminary X-ray powder diffraction analyses (XRD) for identification of serpentine minerals were made using a Rigaku Geigerflex RAD3-C with Ni-filtered CuK radiation. For accurate measurement of d-spacing for serpentine samples, XRD patterns were recorded by step scan mode. Step interval and counting time were 0.02°(2θ) and 2 seconds, respectively. Slit set was 0.5°-0.15㎜-1°.

Polished thin sections were carbon-coated for electron microprobe analysis (EPMA). Quantitative chemical analyses were performed by wavelength dispersive X-ray spectrometer (WDS) controlled by a Link Specta System with LIF, PET, and TAP crystals using JEOL JXA 733 Superprobe instrument. Data correction was performed using a standard ZAF correction procedure of Specta software supplied by Link System. The accelerating voltage was 15 kV, the beam current 10 nA, and the spot size 3-4μm.

Scanning electron microscope (SEM) was used for the external morphological and textural study of individual serpentine minerals as well as the grain interfaces with other minerals of talc ore. JEOL JSM 840A fitted with a Link energy-dispersive X-ray (EDS) detector and CAMECA SX50 were used. Back-scattered electron images (BSEI) were obtained with a JEOL JXA 733 Superprobe, fitted with a Link EDS detector.

RESULTS AND DISCUSSION

Occurrence of Serpentinite

In the study area, it is hard to find the relicts of original ultramafic rocks of pre-serpentinization, because they were intensively altered to serpentinite and steatite. Fresh serpentinite is also not abundantly found. It is green to dark green in color and has appearance similar to talc ore containing large amount of impure minerals such as chlorite and/or phlogopite. However, fresh serpentinite is more massive in occurrence and much harder than talc-chlorite rock. Occasionally, fibrous serpentine minerals form small veins of 5 to 10mm in width at the margin of serpentinite body perpendicular to the veins. Under the microscope, serpentinites consist mostly of serpentine minerals (antigorite with small amount of lizardite) with small amounts of olivine, talc, chlorite, magnesite, and other opaque minerals such as chromite and magnetite. They often show magnetite network structure, which was formed by during olivine → antigorite reaction.

Fresh serpentinites containing large amount of olivine are usually massive in texture and dark green to black in color. It is observed under the microscope that antigorite is mainly formed along the margins or fractures of olivine grains, occasionally resulting in magnetite network texture. It is also observed that pseudomorphs or relicts of olivine are preserved in serpentinite. Greenish black bands or dots seen in hand specimens of serpentinite are composed mostly of olivine under the microscope. Fig. 3 shows serpentinization of ultramafic rocks. Zone 1 consists of olivine + antigorite (Fig. 3B). Zone 2, adjacent to the zone 1, is composed of antigorite + magnesite without olivine (Fig. 3C).

Mineralogy and Chemistry of Serpentine Minerals

XRD study indicates that antigorite is the most abundant serpentine mineral in the study area, even though it is known that it is next in abundance to lizardite in nature. However, lizardite also occurs frequently. The XRD pattern of serpentine mineral is shown in Fig. 4. It was identified as antigorite by the (330) reflection at 1.559Å, which is unique reflection of antigorite (Wicks and O'Hanley, 1988).

Lizardite and chrysotile are true polymorphs with the ideal serpentine formula, $Mg_6Si_4O_{10}(OH)_8$, whereas antigorites are slightly SiO_2-rich and MgO-, OH-poor owing to the alternating wave structure of antigorite (Kunze, 1961; Whitaker and Wicks, 1970;

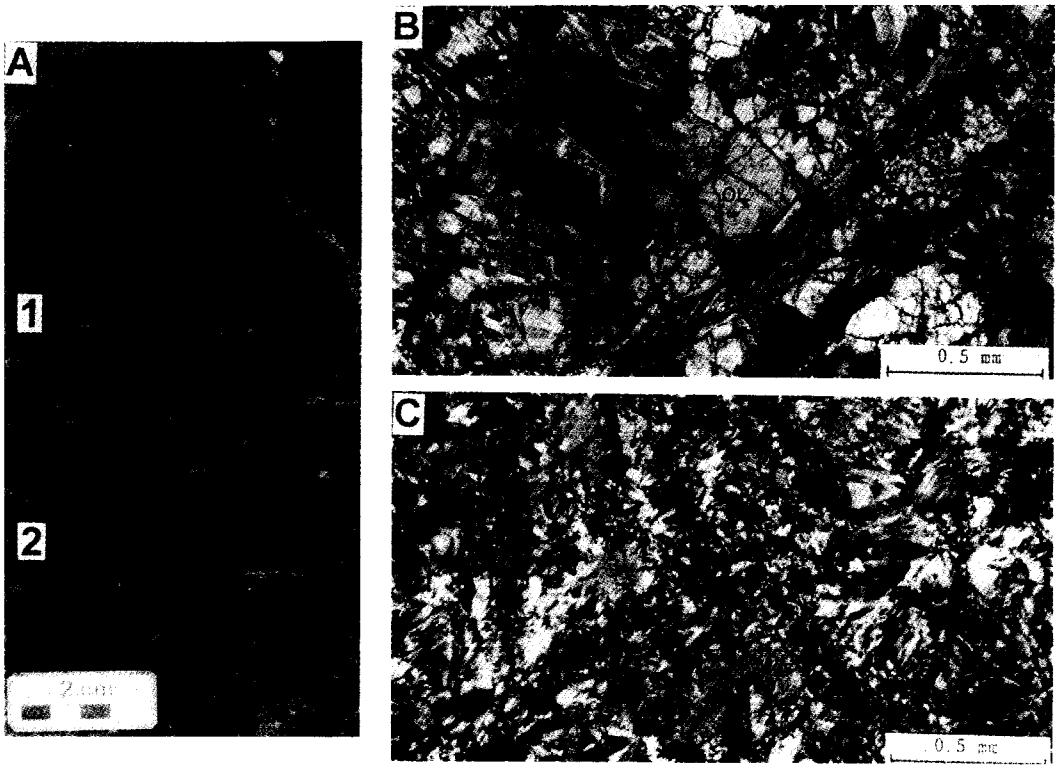

Fig. 3. (A) Photograph of fresh serpentinite (sample T-4) illustrating times of antigorite serpentinization events. Zone 1 (more dark-colored part) consists of rusty olivine hydrated partially to antigorite. Zone 2 consists of antigorite. (B) Photomicrograph of zone 1 showing the replacement of olivine (Ol) by antigorite. A large amount of relicts of olivine preserved in the dark green part of serpentinite. (C) Photomicrograph of zone 2 showing antigorite + magnesite (Mgs).

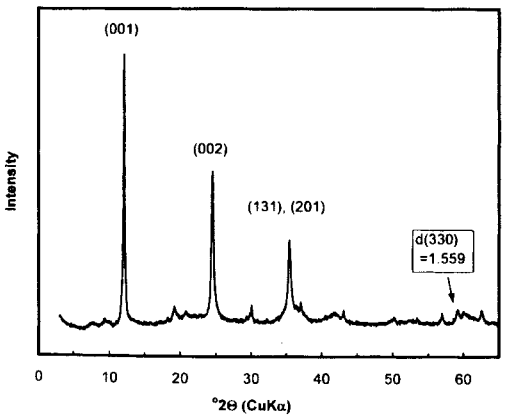

Fig. 4. XRD pattern of representative antigorite (sample R-17). The unique (330) reflection of antigorite is marked by arrow.

Peacock, 1987). Electron microprobe analyses (EPMA) were carried out to know the chemistry of serpentine and the representative data are presented in Table 1. The chemical differences between antigorite and lizardite/chrysotile are small, so both minerals cannot be easily discernible with the electron microprobe. Structural formula of serpentines in Table 1 was normalized to 7 oxygens.

Chemical composition of serpentine is controlled in part by the bulk composition of the original ultrabasic rock from which it has formed. Fe content of serpentine in fresh serpentinites is lower than those in the talc ores or altered serpentinites (Fig. 5), suggest-suggesting that some Fe was introduced into

Table 1. Representative electron microprobe analyses of serpentine.

Sample #	E-22	R-17	Q-9	P-8	P-12-1	P-12-2	P-16	B-30	C-2	C-11	C-28	Q-5	Q-6-2	Q-9	C-44
*(N)	(4)	(12)	(11)	(9)	(2)	(17)	(4)	(10)	(10)	(3)	(8)	(12)	(1)	(12)	(11)
SoO_2	41.68	41.01	45.11	40.38	44.82	41.46	42.73	42.09	41.11	42.32	42.14	42.06	42.68	42.29	42.16
Al_2O_3	2.20	3.10	0.38	1.89	0.96	2.13	1.14	1.81	2.08	1.14	1.23	2.24	0.95	1.66	3.27
TiO_2	0.01	0.03	0.02	0.01	0.01	0.02	0.02	0.03	0.01	0.00	0.01	0.02	0.00	0.01	0.04
Cr_2O_3	0.31	0.37	0.02	0.15	0.07	0.09	0.12	0.17	0.63	0.28	0.13	0.19	0.10	0.08	0.50
NiO	0.18	0.15	0.12	0.21	0.16	0.15	0.17	0.23	0.14	0.14	0.10	0.16	0.15	0.15	0.10
FeO	6.54	1.94	6.60	10.33	6.64	7.38	8.60	8.34	5.84	6.73	5.74	10.61	9.29	6.56	7.18
MgO	33.66	37.66	35.10	30.88	30.87	32.75	32.93	33.94	33.72	34.01	34.91	32.13	33.35	35.06	33.59
MnO	0.01	0.05	0.10	0.09	0.05	0.04	0.01	9.11	0.03	0.04	0.01	0.12	0.07	0.06	0.90
CaO	0.02	0.01	0.00	0.02	0.01	0.04	0.03	0.03	0.01	0.01	0.02	0.01	0.01	0.03	0.02
Na_2O	0.00	0.00	0.01	0.01	0.03	0.02	0.00	0.01	0.01	0.01	0.01	0.01	0.00	0.00	0.01
K_2O	0.00	0.01	0.01	0.00	0.00	0.01	0.00	0.00	0.02	0.02	0.03	0.01	0.00	0.00	0.01
TOTAL	84.60	84.34	87.47	83.98	83.61	84.10	85.75	86.76	83.59	84.69	84.32	87.56	86.59	85.91	86.97
Si	2.03	1.97	2.12	2.03	2.19	2.04	2.08	2.02	2.03	2.06	2.05	2.02	2.06	2.03	2.01
Al(Ⅳ)	0.00	0.06	0.00	0.01	0.00	0.02	0.00	0.02	0.03	0.00	0.00	0.03	0.00	0.01	0.03
Sum	2.04	2.03	2.12	2.04	2.19	2.06	2.08	2.04	2.05	2.06	2.05	2.05	2.06	2.04	2.04
Al(Ⅳ)	0.12	0.11	0.02	0.10	0.06	0.11	0.07	0.09	0.10	0.07	0.07	0.10	0.05	0.09	0.15
Ti	0.00	0.00	0.00	0.00	0.00	0.00	0.00	0.00	0.00	0.00	0.00	0.00	0.00	0.00	0.00
Cr	0.01	0.01	0.00	0.01	0.00	0.00	0.00	0.01	0.02	0.01	0.00	0.01	0.00	0.00	0.02
Ni	0.01	0.01	0.00	0.01	0.01	0.01	0.01	0.01	0.01	0.01	0.00	0.01	0.01	0.01	0.00
[b]Fe	0.27	0.08	0.26	0.43	0.27	0.30	0.35	0.34	0.24	0.27	0.23	0.43	0.38	0.26	0.29
Mg	2.45	2.69	2.46	2.31	2.25	2.41	2.38	2.43	2.48	2.47	2.54	2.31	2.40	2.51	2.38
Mn	0.00	0.00	0.00	0.00	0.00	0.00	0.00	0.00	0.00	0.00	0.00	0.00	0.00	0.00	0.00
Ca	0.00	0.00	0.00	0.00	0.00	0.00	0.00	0.00	0.00	0.00	0.00	0.00	0.00	0.00	0.00
Na	0.00	0.00	0.00	0.00	0.00	0.00	0.00	0.00	0.00	0.00	0.00	0.00	0.00	0.00	0.00
K	0.00	0.00	0.00	0.00	0.00	0.00	0.00	0.00	0.00	0.00	0.00	0.00	0.00	0.00	0.00
Sum	2.86	2.91	2.75	2.87	2.59	2.83	2.81	2.88	2.85	2.83	2.85	2.86	2.85	2.88	2.85

[a]Number of analysis

[b]All Fe calculated as Fe^{2+}

serpentinite by hydrothermal solution during steatitization. As shown in Table 1, nickel and chrome are always minor or trace components of serpentine minerals because they were minor components of the initial rock and remained dispersed throughout the rock during serpentinization.

Textures of Serpentine Minerals

If ultramafic rocks were subjected to deformation at various times, that is, prior to, during and after serpentinization, some of these events are recorded in the serpentine minerals that make up of the rocks. Wicks et al. (1977), Wicks and Whittaker (1977), and Wicks and Plant (1979) described a variety of serpentine-mineral textures from serpentinized ultramafic rocks in different geological environments.

In spite of intensive serpentinization and steatitization, it can be seen that the

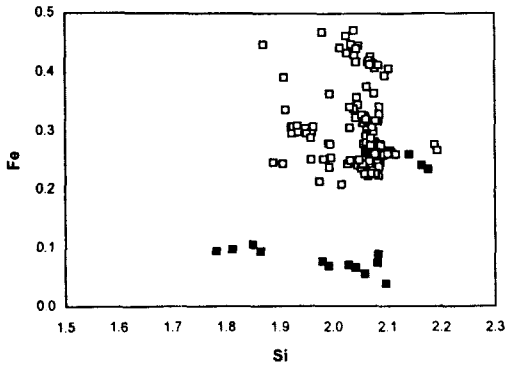

Fig. 5. Compositions of serpentine minerals in Si versus Fe (based on 7 oxygens). Filled square : serpentine minerals from fresh serpentinite, Open square : serpentine minerals from altered serpentinite or talc ores.

serpentinite in the study area preserves more or less the textures of olivine and minor enstatite. Careful examination of the serpentine pseudomorphic textures reveals that the parent rock of the serpentinite composed mainly of olivine with minor pyroxene and amphibole. It is often observed that pseudomorphic replacement of olivine by serpentine along grain boundaries and fractures produces a characteristic polygonal cell texture (Fig. 6A). The morphology of the pseudomorphs indicates that the olivine phenocrysts were subhedral to euhedral. Each cell has a central zone consisting of relict olivine. The presence of relict phases indicates incomplete serpentinization reaction by not enough availability of H_2O. Such olivine relicts in serpentinite commonly show evidence of

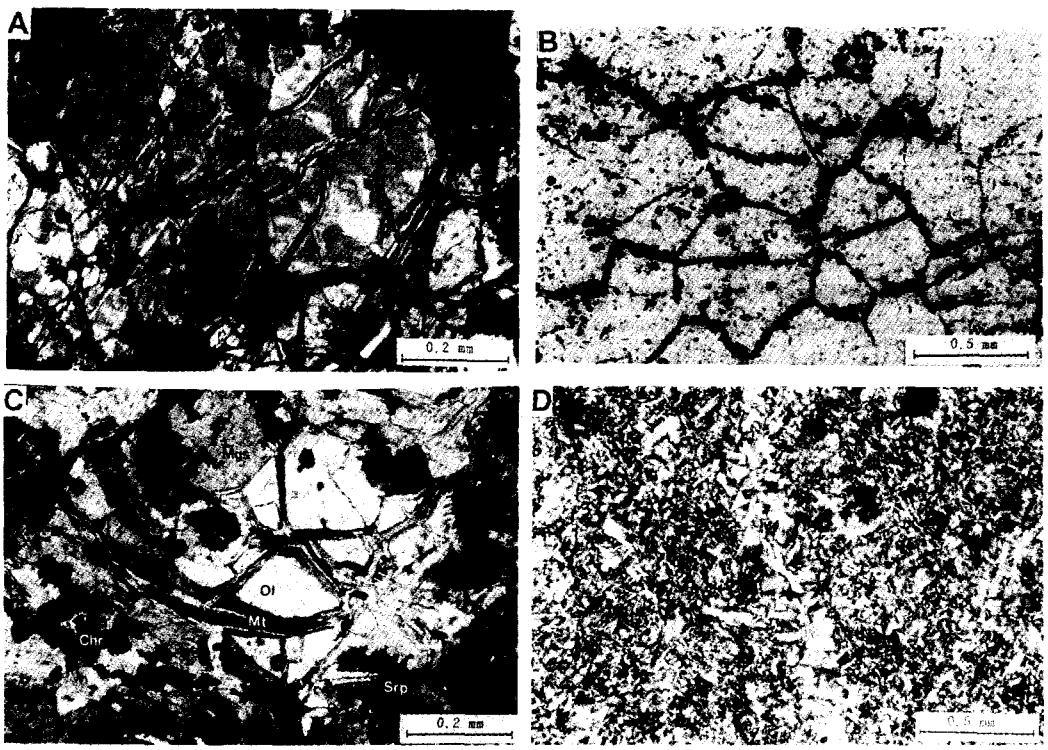

Fig. 6. (A) Photomicrograph of olivine showing alteration to serpentine along grain boundaries and fractures to produce a characteristic polygonal cell texture. Each cell has a central zone consisting of relict olivine or of serpentine. (B) Magnetite (opaque) networks formed by the olivine → antigorite reaction in serpentinite (sample R-17). Plane polarized light. (C) Serpentine pseudomorphic texture with relict olivine centers (sample T-4-4). (D) Interpenetrating texture in antigorite-rich rock (sample Q-14).

alteration events. Large fractures that are filled with fine-grained serpentine and opaque minerals occur throughout the grains suggesting early fracturing and alteration (Figs. 6B, 6C). In some cases, back-scattered electron micrograph of fresh serpentinite shows fractures formed within the central olivine grain (Fig. 7B) after main serpentinization.

The pseudomorphic replacement of olivine and pyroxene by serpentine occurs during retrograde serpentinization (Wicks and Whittaker, 1977). Most pseudomorph in serpentinite from the study area are composed of lizardite as evidenced by lattice-fringe image under TEM (Kim, 1997). Lizardite commonly shows pseudomorphic textures after olivine (Figs. 6B, 6C, 7). Scanning electron microscope (SEM) study indicates that most serpentine minerals occur as platy or tabular form (Fig. 8A) rather than asbes-tiform (Fig. 8B). In some cases, poorly crystallized talcs of 2-3 m in size which have been formed by alteration of well-crystallized serpentine minerals are associated with serpentine minerals (Fig. 8C). Such talc and serpentine minerals can be distinguished by intensity ratios of Mg/Si in EDS patterns (Figs. 8D, 8E).

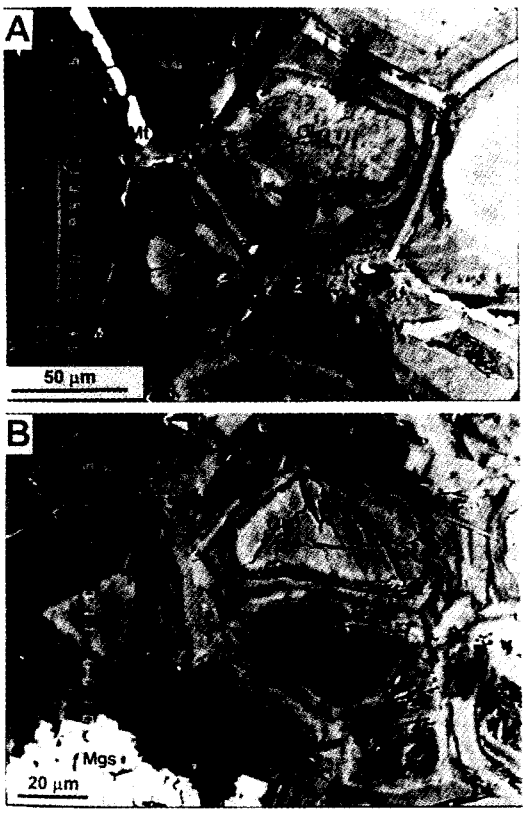

Fig. 7. Back-scattered electron micrographs of fresh serpentinite. (A) Alteration of olivine to antigorite resulting in the serpentine pseudomorphic texture with magnetite network along original olivine grain boundaries. (B) Serpentine pseudomorphic texture with relict olivine and magnesite. Fractures formed after major serpentinization stage are observed in central olivine grain. Original grain boundaries of parent olivine are preserved. Ol : olivine, Srp : serpentine, Mt : magnetite, Mgs : magnesite.

Secondary magnetite associated with the serpentinization is commonly found along the former olivine grain boundaries and fractures showing network textures (Figs. 6B, 6C, 7A). However, the presence of brucite in association with lizardite is not detected suggesting no excess content of Mg over the ideal serpentine chemistry (Table 1). Minor amounts of chrysotile do occur together with lizardite, particularly in some samples of pyroxene bastite, but it is not a major phase in pseudomorphs in the retrograde environment. Lizardite stains readily to an orange-brown color during weathering and has a slightly higher index of refraction than antigorite (Figs. 9B, 9D).

Slightly serpentinized olivine grains are often preserved in serpentinite (Fig. 6C). With increasing serpentinization, antigorite blades penetrated into the olivine subgrains, in contrast to the pseudomorphic texture formed by lizardite after olivine. Crude lens-shaped pseudomorphs of antigorite after olivine are resulted from incomplete serpentinization (Fig. 9A).

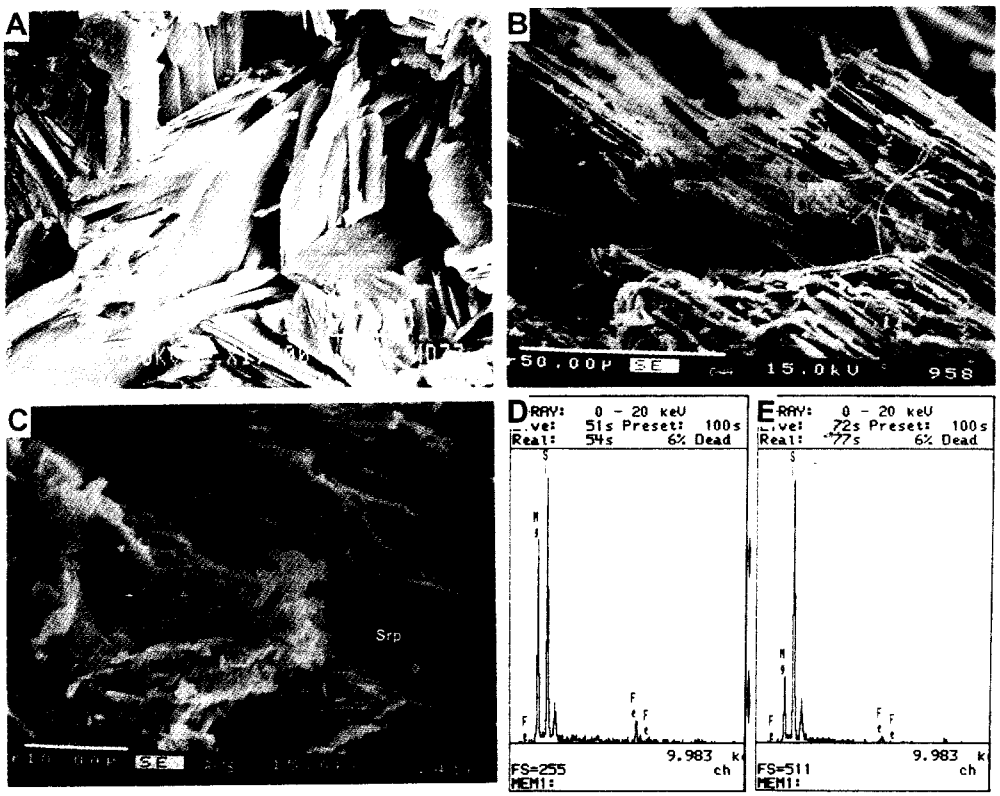

Fig. 8. Scanning electron micrographs (A,B,C) of serpentine. (A) Flaky and tabular crystals of serpentine. (B) Asbestiform serpentine. (C) Poorly crystallized talc and altered serpentine. EDS pattern of serpentine (D) and talc (E) of (C). Talc and serpentine can be distinguished by intensity ratio of Mg/Si in EDS patterns.

Most of serpentinites usually show non-pseudomorphic interpenetrating texture by antigorite which shows elongate blades, flakes, or plates (Fig. 6D) obliterating previous textures. Antigorite only rarely forms pseudomorphs of other minerals (Wicks and O'Hanley, 1988). Compared to lizardite and chrysotile, antigorite is relatively unsusceptible to discoloration by weathering (Peacock, 1987) and the orientation of the elongate grains is completely random, resulting in massive serpentinite. Therefore, the serpentinite composed mainly of antigorite is usually massive in appearance and green to dark green in color. The pseudomorphic and non-pseudomorphic textures of serpentines are found independently or together showing gradational features. Some of the pseudomorphic texture of antigorite and lizardite (Figs. 7, 9) are formed in an early stage in the development of interpenetrating texture (Fig. 6D).

Serpentinization

Careful observation of the serpentine textures gives a great deal of data on the pre-serpentinization nature of the ultramafic rocks and their process of serpentinization. The serpentinization might begin from the ultramafic protolith, which is most probably

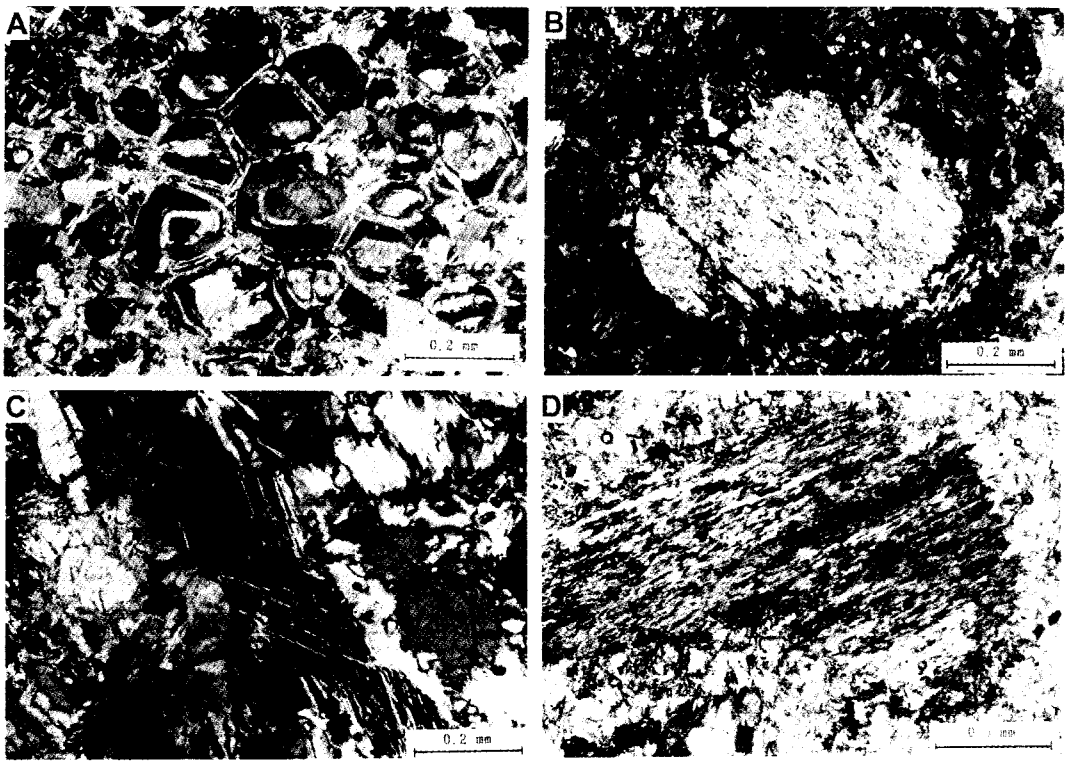

Fig. 9. (A) Replacement of olivine by antigorite to produce crude lens-shaped pseudomorphs (sample P-12). (B) Lizardite (apparent fibers) bastite after orthopyroxene in the matrix of interpenetrating texture of antigorite (sample E-22). (C) Replacement of clinopyroxene or amphibole by lizardite along cleavages (sample R-17). (D) Possible antigorite bastite of uncertain origin (sample T-3-3).

dunite, peridotite, or olivine gabbro, which are assemblages of olivine and some other mafic minerals such as enstatite.

Olivine is the major parent mineral of serpentine. It usually occurs as anhedral grains embedded in a groundmass of serpentine minerals. The outline of original large olivine grains can be traced by the optical continuity of small olivine grains separated by secondary serpentine minerals. The microprobe analyses show a limited chemical composition from Fo90 to Fo93. (Table 2). Such chemical homogeneity of olivine indicates a chemically homogeneous ultramafic rock as the parent rock of serpentinite.

If the ultramafic bodies with a small concentration of enstatite is tectonically emplaced, the first reaction will be the retrograde hydration of this originally high temperature-pressure assemblage in response to the lower temperature environment of relatively wet condition. There are several problems in the interpretation of the serpentinization process, among which the most difficult problem is the source of water to produce the serpentine. Hess (1936) suggested that serpentinization is an autometamorphic alteration which occurs during the last stage of the intrusion of the ultrabasic. However, because it is very unlikely that during intrusion the hot

Table 2. Electron microprobe analyses of olivine.

POINT	100	102	104	106	107	112	114	116	118	122	124	125	126	132	133	137	169	176
SiO_2	40.55	40.94	40.50	40.61	41.25	40.64	40.44	41.14	41.29	40.81	41.00	41.42	40.63	40.99	40.54	40.74	40.35	40.96
Al_2O_3	0.00	0.00	0.00	0.00	0.00	0.00	0.00	0.00	0.00	0.00	0.00	0.17	0.00	0.00	0.00	0.00	0.00	0.00
TiO_2	0.00	0.00	0.00	0.00	0.00	0.00	0.00	0.00	0.00	0.00	0.00	0.01	0.00	0.00	0.00	0.00	0.00	0.00
Cr_2O_3	0.00	0.01	0.00	0.04	0.00	0.05	0.00	0.00	0.02	0.00	0.00	0.03	0.00	0.00	0.01	0.02	0.00	0.03
NiO	0.34	0.38	0.38	0.28	0.38	0.33	0.31	0.34	0.30	0.38	0.31	0.32	0.38	0.44	0.45	0.38	0.27	0.37
FeO	8.76	8.68	8.92	9.00	8.95	8.89	8.90	9.31	9.08	8.94	9.16	6.84	9.21	8.90	8.90	9.23	9.906	8.86
MgO	49.25	49.55	49.32	49.46	49.18	49.49	49.43	49.59	49.75	49.42	49.16	49.95	48.96	48.92	49.25	49.01	49.17	49.44
MnO	0.14	0.23	0.18	0.20	0.17	0.19	0.17	0.20	0.18	0.15	0.14	0.69	0.11	0.18	0.09	0.16	0.17	0.21
CaO	0.00	0.00	0.00	0.00	0.01	0.01	0.00	0.01	0.00	0.01	0.04	0.10	0.00	0.01	0.02	0.00	0.00	0.01
Na_2O	0.00	0.00	0.00	0.00	0.01	0.00	0.00	0.00	0.00	0.00	0.00	0.00	0.00	0.00	0.00	0.00	0.00	0.02
K_2O	0.00	0.00	0.00	0.00	0.00	0.00	0.00	0.00	0.00	0.00	0.00	0.00	0.00	0.00	0.00	0.00	0.00	0.00
Total	99.04	99.78	99.29	99.59	99.93	99.60	99.25	100.59	100.61	99.71	99.80	99.54	99.29	99.42	99.26	99.53	99.02	99.90
								cations per 4 oxygens										
Si	1.00	1.00	1.00	1.00	1.01	1.00	1.00	1.00	1.00	1.00	1.00	1.01	1.00	1.01	1.00	1.00	1.00	1.00
Al	0.00	0.00	0.00	0.00	0.00	0.00	0.00	0.00	0.00	0.00	0.00	0.00	0.00	0.00	0.00	0.00	0.00	0.00
Ti	0.00	0.00	0.00	0.00	0.00	0.00	0.00	0.00	0.00	0.00	0.00	0.00	0.00	0.00	0.00	0.00	0.00	0.00
Cr	0.00	0.00	0.00	0.00	0.00	0.00	0.00	0.00	0.00	0.00	0.00	0.00	0.00	0.00	0.00	0.00	0.00	0.00
Ni	0.01	0.01	0.01	0.01	0.01	0.01	0.01	0.01	0.01	0.01	0.01	0.01	0.01	0.01	0.01	0.01	0.01	0.01
[b]Fe	0.18	0.18	0.18	0.18	0.18	0.18	0.18	0.19	0.18	0.18	0.19	0.14	0.19	0.18	0.18	0.19	0.19	0.18
Mg	1.81	1.81	1.81	1.81	1.79	1.81	1.81	1.80	1.80	1.81	1.79	1.81	1.80	1.79	1.81	1.80	1.81	1.80
Mn	0.00	0.00	0.00	0.00	0.00	0.00	0.00	0.00	0.00	0.00	0.00	0.00	0.00	0.00	0.00	0.00	0.00	0.00
Ca	0.00	0.00	0.00	0.00	0.00	0.00	0.00	0.00	0.00	0.00	0.00	0.00	0.00	0.00	0.00	0.00	0.00	0.00
Na	0.00	0.00	0.00	0.00	0.00	0.00	0.00	0.00	0.00	0.00	0.00	0.00	0.00	0.00	0.00	0.00	0.00	0.00
K	0.00	0.00	0.00	0.00	0.00	0.00	0.00	0.00	0.00	0.00	0.00	0.00	0.00	0.00	0.00	0.00	0.00	0.00
Sum	2.00	2.00	2.01	2.01	1.99	2.00	2.01	2.00	1.99	2.00	1.99	1.98	2.00	1.99	2.00	2.00	2.01	2.00
Mg	90.9	91.1	90.8	90.7	90.7	90.8	90.8	90.5	90.7	90.8	90.5	92.9	90.4	90.7	90.8	90.4	90.6	90.0
Fe	9.1	8.9	9.2	9.3	9.3	9.2	9.2	9.5	9.3	9.2	9.5	7.1	9.6	9.3	9.2	9.6	9.4	9.1

[b]All Fe calculated as Fe

ultramafic rock contained the 14 wt.% interstitial water required for serpentinization (Frances 1956), the water from magma itself is not suitable source for serpentinization. Therefore, if serpentinization is the autometasomatic alteration, the water must have been picked up by the magma from the relatively wet country rock with which ultramafic came in contact during its intrusion. Deep-seated basic intrusions into the water-bearing country rocks might have, and almost inevitably would have a lower vapor pressure than the wall rocks, and then the magma would absorb water from the surrounding rocks. The absence of contact metamorphism around serpentinite in the study area favors the hypothesis that the solutions were moving from the country rocks into the magma. However, the water content of the granitic gneiss is low, so that this interpretation is not enough to explain the vast amount of water to produce the large serpentinite body.

Another possible water source is the deep-seated hydrothermal serpentinizing solution (Grubb, 1962). The hydrothermal solution could have been slowly acquired from the fault and fracture system over a

long period of time (Wenner and Taylor, 1971; Barnes and O'Neil, 1969). Concerning the source of water for serpentinization, any interpretation stated above, as a single origin, could not be a ready source of water. Thus, it is considered that the serpentinization took place by autometamorphism at early stage and by hydrothermal alteration at late stage.

Lack of minerals other than serpentine as well as magnesite and rarely chromite in serpentinite from the study area indicates that the solution was relatively pure silicic water and there was little gain or loss of elements during serpentinization. The only phase added to the ultramafic body was water during critical stages of its cooling. The reactions expected to have occurred for the formation of serpentinite from ultramafic rocks might probably be the following two equations.

$$3Mg_2SiO_4 + SiO_2 + 4H_2O \rightarrow 2Mg_3Si_2O_5(OH)_4$$
forsterite → serpentine

$$Mg_2SiO_4 + MgSiO_3 + 2H_2O \rightarrow Mg_3Si_2O_5(OH)_4$$
forsterite + enstatite → serpentine

CONCLUSIONS

Serpentinite from the Yesan-Gongju-Cheongyang area has been formed by serpentinization of ultramafic rock. The mineralogical characters of serpentine minerals have been studied using X-ray diffraction analysis, and various electron microscopy such as EPMA and SEM. The serpentinization process of ultramafic rocks have been interpreted by textural evidences of serpentine minerals.

Serpentine minerals occur not only as major mineral of serpentinite, but also as remnants in the talc ore. XRD study indicates that antigorite is the most abundant serpentine mineral of serpentinite. Antigorite was mainly formed along the margins or fractures of olivine grains occasionally resulting in the formation of magnetite network texture. Lizardite shows pseudomorphic texture.

Careful examination of the serpentine textures reveals that the parent rock of the serpentinite was mainly composed of olivine with minor pyroxene. Replacement relicts of olivine are found in serpentinites. The microprobe analyses show a very narrow compositional variation ranging from Fo90 to Fo93. Such chemical homogeneity of olivine indicates a chemically homogeneous ultramafic rock as the parent rock of serpentinite.

Serpentinite consisting of antigorite usually shows non-pseudomorphic texture, whereas that consisting of lizardite shows pseudomorphic texture in which the parent grain boundaries were preserved. The antigorite shows elongate blades, flakes, or plates that form a tight interpenetrating texture obliterating the previous textures. Lizardite commonly forms pseudomorphic textures after olivine and also occurs as replacement of pyroxene. In some cases, fractures formed after main serpentinization are observed within the central olivine grain.

Careful observation of the serpentine pseudomorphs gives a great deal of data on the pre-serpentinization nature of the ultramafic rocks. The ultramafic body may have intruded along a major fault, which can be inferred by the linear form of present ore body. Once the emplacement of ultramafic body into the relatively wet environment ceased and the cooling intrusive body crossed into the stability field of serpentine, serpentinization of the olivine and pyroxene took place. The pervasive serpentinization of whole ultramafic body occurred at the later time with enough water of external source. Lack of minerals other than serpentine as well as magnesite and rarely chromite in serpentinite from the study area indicates that the solution was relatively pure silicic water and there was little gain or loss of elements during serpentinization. It is inferred that the final pervasive serpentinization took place over a long time, possibly with hydrothermal water supplied from the fracture system produced during emplacement of ultramafic rock.

ACKNOWLEDGMENTS

This study was carried out by the BSRI project 96-5404 funded by the Ministry of Education, Korea.

REFERENCES

Barnes, I. and O'Neil, J. R. (1969) The relationship between fluids in some fresh alpine-type ultramafics and possible modern serpentinization, western United States. Geol. Soc. Amer. Bull. 80, 1947-1960.

Boyd, F. R. and Nixon, P. H. (1979) Garnet iherzolite xenoliths from the kimberlites of East Griqualand, South Africa. Carnegie Inst. Wash. Yearbook, 78, 488-492.

Francis, G. H. (1956) The serpentinite mass in Glen Uruquhart, Invernesshire, Scotland. Am. Jour. Sci., 254, 201-226.

Grubb, P. L. C. (1962) Serpentinization and chrysotile formation in the Matheson ultrabasic belt, northern Ontario. Econ. Geol., 57, 1228-1246.

Hess, H. H. (1933) The problem of serpentinization and the origin of certain chrysotile asbestos talc and soapstone deposits. Econ. Geol., 28, 634-657.

Jago, B. C. and Mitchell, R. H. (1985) Mineralogy and petrology of the Ham kimberlite, Somerset Island, Northwest Territories. Can. Mineral., 23, 619-633.

Kim, G.-Y. (1997) Electron Microscopic Study on the Talc Mineralization in the Yesan-Gongju-Cheongyang Area, Korea. Ph.D thesis.

Kunze, G. (1961) Antigorite. Strukturtheoretische Grundlagen und ihre praktische Bedeutung F r die weitere Serpentin-Forschung. Fortsche. Mineral., 39, 206-324.

Laurent, R. and Hebert, Y. (1979) Paragenesis of serpentine assemblages in harzburgite tectonite and dunite cumulate from the Quebec Appalachians. Can. Mineral., 17, 857-869.

Lee, S. H. and Choi, G. J. (1994) Geochemistry and chemical equilibria of coexisting minerals in the gneisses around the Daeheung Talc Deposits, Korea, Jour. Petrol. Soc. Korea, 3, 138-155. (in Korean).

Mitchell, R. H. (1986) Kimberlites: mineralogy, geochemistry, and petrology. Plenum, New York.

Mitchell, R. H. and Putnis, A. (1988) Polygonal serpentine in segregation-textured kimberlite. Can. Mineral., 26, 991-997.

Peacock, S. M. (1987) Serpentinization and infiltration metasomatism in the Trinity peridotite, Klamath province, northern California: implications for subduction zones. Contrib. Mineral. Petrol., 95, 55-70.

Sharp, T. G., Otten, M. T., and Buseck, P. R. (1990) Serpentinization of phlogopite phenocrysts from a micaceous kimberlite. Contrib. Mineral. Petrol., 104, 530-539.

Wenner, D. B. and Taylor, H. P., Jr. (1971) Temperatures of serpentinization of ultramafic rocks based on O18/O16 fractionation between coexisting serpentine and magnetite. Contrib. Mineral. Petrol., 32, 165-185.

Whittaker, E. J. W. and Wicks, F. J. (1970) Chemical differences among the serpentine "polymorphs": a discussion. Am. Mineral., 55, 1025-1047.

Wicks, F. J. (1984) Deformation histories as recorded by serpentinites. I. Deformation prior to serpentinization. Can. Mineral. 22, 185-195.

Wicks, F. J. and O'Hanley, D. S. (1988) Serpentine minerals: Structures and petrology. In: Bailey, S. W., Ed., Hydrous Phyllosilicates, Reviews in Mineralogy, Vol. 19, Mineralogical Society of America, 91-167.

Wicks, F. J. and Plant, A. G. (1979) Electron microprobe and X-ray microbeam studies of serpentine textures. Can. Mineral. 17, 785-830.

Wicks, F. J. and Whittaker, E. J. W. (1977) Serpentine textures and serpentinization. Can. Mineral. 15, 459-488.

Wicks, F. J., Whittaker, E. J. W., and Zussman, J. (1977) An idealized model for serpentine textures after olivine. Can. Mineral. 15, 446-458.